단순 인장 실험에 의한 외부 스티프너를 갖는 각형 강관기둥과 H형강보 접합부의 최대내력에 대한 연구

A Study on the Strength of H Beam-to-Rectangular Tube Column Connections with Exterior Diaphragms by Simplified Tension Test

박 종 원[1] · 강 해 관[2] · 이 상 훈[3] · 김 영 찬[4]
Park, Jong Won Kang, Hae Kwan Lee, Sang Hoon Kim, Young Chan

요 약 : 각형 강관 기둥과 H형 보의 접합부에 대한 연구는 보의 하중을 기둥에 전달하는 과정에서 생기는 응력의 집중현상 때문에 하중을 효율적으로 전달하는 방식을 고안하는 것에 초점을 맞추었다. 본 연구에서는 외부보강형 접합부의 강도를 증가시키기 위한 방법으로 직사각형의 스티프너를 사용하였다. 실물의 절반크기로 시험체를 제작하여 단순 인장실험을 실시하였다. 항복선이론과 가상일법을 이용하여 접합부의 극한강도를 추정하는 공식을 유도하였으며 실험치에 근접한 결과를 얻었다.

ABSTRACT : A moment connection of H beam-to-rectangular tube column with external stiffeners was proposed. A formula to predict the ultimate strength of the connection was derived based on the yield line mechanism. Experimental investigation was performed to determine the applicability of the connection type and the strength formula. The ultimate strengths computed by the formula agreed well with the experimental values.

핵 심 용 어 : 각형 강관, 기둥-보 접합부, 외부스티프너
KEYWORDS : Rectangualr steel tube, beam-to-column connection, simplified tension model, ultimate strength prediction, exterior stiffener

1. Introduction

The use of structural tube sections has been increased significantly because of the superior column performance such as large radius of gyration about each axis

1) 홍익대학교 건축공학과 조교수
2) 서울대학교 건축학과 박사수료
3) 서울대학교 건축학과 석사과정
4) 부경대학교 건축공학과 전임강사

본 논문에 대한 토의를 1998년 9월 30일까지 학회로 보내주시면 토의 회답을 게재하겠습니다.

and high torsional rigidity.

Either rectangular or circular tube section allows easy beam-to-column connections for simple supports. However, for moment connections, rectangular tube sections provide more convenient shapes.

Research has been carried out on different types of moment connections of H beam-to-rectangular tube column. They range from the running of continuity plates through or around the tube column to the provision of diaphragms inside the tube or flange diaphragms around the tube[1,2].

In this study, a moment connection with external stiffeners is proposed and tests are performed. Based on the yield line mechanism, a formula to predict the ultimate strength of the connection is derived. Experimental and analytical results are compared to verify the applicability of the formula within engineering accuracy.

2. Experimentation

2.1 Test Specimens

The material properties of steel and concrete were obtained from coupon and cylinder tests. The strength of materials is shown in Table 1.

Table 1. Material Property

Material		Thickness (mm)	Strength(t/cm²)	
			Yield	Ultimate
Steel	Column	5	4.05	4.73
		6	4.67	5.28
		9	3.99	4.92
	Stiffener	9	3.37	5.27
		12	2.92	4.64
		15	2.70	4.76
		18	3.70	5.54
Concrete(F_c', kg/cm²)			261.7	

Specimens were classified as C-, E- and S-types according to the eccentricity of

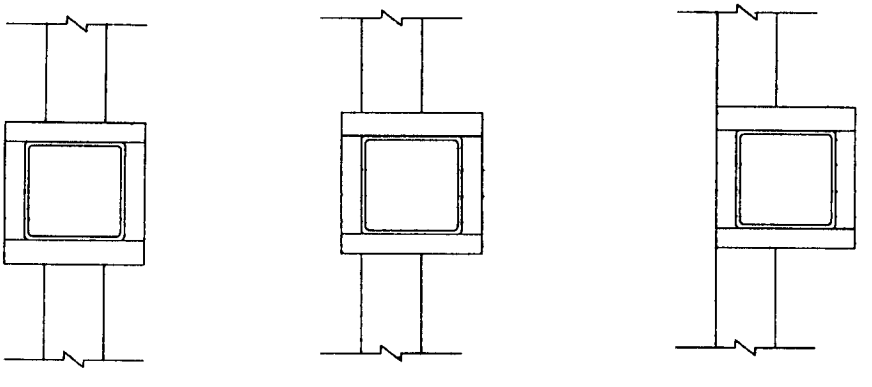

(a) C TYPE (b) E TYPE (c) S TYPE

Fig. 1 Type of Test Specimens

the beam flange from the centerline of the column flange as shown in Figure 1. C-type connection was proposed for interior columns. E- and S-type connections were for exterior columns. The configuration of specimens for the C-type connection is illustrated in Figure 2. The dimensions of test specimens are listed in Table 2. One specimen without stiffener and one specimen with flange diaphragms were tested for comparison.

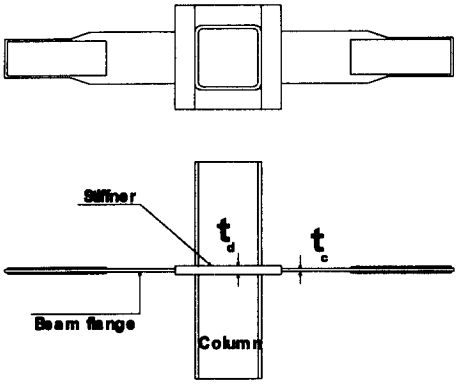

Fig. 2 Configuration of Specimen (unit : mm)

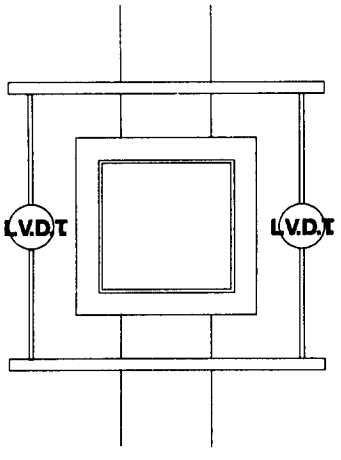

Fig. 3 Displacement Measuring Device

Table 2. Specimen List

Specimen	B_c	t_c	B_f	t_f	h_d	t_d	$h_{d''}$
C15N-12B	250	6	150	12	25	15	25
C15M-12B	250	6	150	12	50	15	50
C15W-12B	250	6	150	12	75	15	75
C12M-12B	250	6	150	12	50	12	50
C18M-12B	250	6	150	12	50	18	50
C15M-12A	250	6	100	12	50	15	50
C15M-12C	250	6	200	12	50	15	50
C15M-12B5	250	5	150	12	50	15	50
C15M-12B9	250	9	150	12	50	15	50
C18W-12B	250	6	150	12	75	18	75
C15M-9A	250	6	100	9	50	15	50
C15M-9B	250	6	150	9	50	15	50
C15W-9B	250	6	150	9	75	15	75
C15WN-12B	250	6	150	12	75	15	25
C15WM-12B	250	6	150	12	75	15	50
C15N-12BF	250	6	150	12	25	15	25
C15M-12BF	250	6	150	12	50	15	50
E15N-12B	250	6	150	12	25	15	25
E15M-12B	250	6	150	12	50	15	50
E15W-12B	250	6	150	12	75	15	75
E12M-12B	250	6	150	12	50	12	50
E18M-12B	250	6	150	12	50	18	50
E15M-12A	250	6	100	12	50	15	50
E15M-12C	250	6	200	12	50	15	50
E15WN-12B	250	6	150	12	75	15	25
E15WM-12B	250	6	150	12	75	15	50
E15M-12BF	250	6	150	12	50	15	50
E15W-12BF	250	6	150	12	75	15	75
S15N-12B	250	6	150	12	25	15	25
S15M-12B	250	6	150	12	50	15	50
S15W-12B	250	6	150	12	75	15	75
S12M-12B	250	6	150	12	50	12	50
S18M-12B	250	6	150	12	50	18	50
S15M-12A	250	6	100	12	50	15	50
S15M-12C	250	6	200	12	50	15	50
N-12B[1)]	250	6	150	12	-	-	-
D12N-12B[2)]	250	6	150	12	25	12	-

Note:

1) Specimen without stiffener
2) Specimen with trapezoidal-shaped exterior stiffener

• Specimen was named as follows :

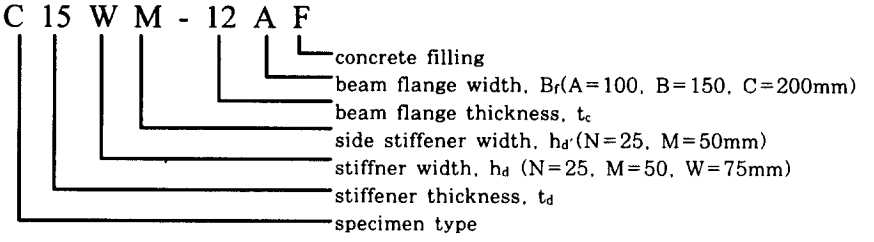

Table 3. Test Result

	P_y (ton)	P_{max} (ton)	δ_y (mm)	δ_{max} (mm)	failure mode
C15N-12B	13.86	29.50	0.53	9.94	A
C15M-12B	28.35	50.90	0.69	5.78	A
C15W-12B	32.27	70.45	0.45	8.46	A
C12M-12B	21.54	39.90	0.69	7.31	A
C18M-12B	29.97	54.25	0.91	8.47	A
C15M-12A	18.49	38.45	0.40	5.65	A
C15M-12C	29.17	56.40	0.44	4.88	A
C15M-9B	24.27	48.30	0.62	9.99	A
C15M-12B5	21.74	38.90	0.51	6.84	A
C15M-12B9	27.04	59.75	0.37	6.41	A
C15M-9A	18.60	40.10	0.40	16.61	C
C15W-9B	33.48	57.10	0.38	11.59	C
C18W-12B	42.37	84.40	0.87	15.50	C
C15WN-12B	27.18	54.75	0.38	7.16	A
C15WM-12B	32.68	58.95	0.76	4.68	A
C15N-12BF	14.92	33.45	0.46	3.90	A
C15M-12BF	22.87	49.05	0.39	15.05	A
E15N-12B	18.50	30.75	0.80	3.36	B
E15M-12B	28.52	50.05	0.87	7.08	B
E15W-12B	35.40	61.55	0.43	6.01	B
E12M-12B	25.14	40.70	0.97	8.38	B
E18M-12B	39.38	69.55	0.91	11.79	A
E15M-12A	26.05	45.40	0.61	7.47	B
E15M-12C	25.98	54.35	0.35	5.56	B
E15WN-12B	31.74	58.90	0.69	13.00	E
E15WM-12B	32.86	65.00	0.52	7.68	B
E15W-12BF	31.69	63.80	0.39	8.38	B
S15N-12B	22.37	53.75	0.61	14.98	A
S15M-12B	36.69	66.85	0.42	8.94	A
S15W-12B	38.18	84.70	0.41	16.81	C
S12M-12B	31.90	59.55	0.39	10.11	B
S18M-12B	44.57	81.40	0.70	16.53	D
S15M-12A	34.94	57.00	0.46	13.72	C
S15M-12C	39.06	74.40	0.54	15.26	A
N-12B	8.65	17.55	3.81	21.2	E
D12N-12B	36.36	82.70	0.16	13.26	D

A : crack in 30° ~45° direction at the joint of stiffener and beam flange
B : crack along the joint of stiffener and beam flange
C : tensile failure of beam flange
D : tensile failure of side stiffener
E : tearing of tube at beam-to-column joint

2.2 Test Procedure

Test was carried out under monotonic tensile loading using UTM. To measure the displacement at the connection, 100 mm displacement transducers were installed as shown in Figure 3. The beam flange and exterior stiffeners were instrumented with electric-resistance strain gauges to investigate the stress concentration.

3. Test Result

Test results are listed in Table 3. Due to the stress concentration and local deformation of the tube, inelastic behavior occurs from the early stage of loading. Therefore, the yield strength P_y is defined as the interseeting point of the initial slope line and the tangent with one third of initial slope of the load-displacement curve. The yield strength(P_y), ultimate strength(P_{max}), displacements at yield(δ_y) and at ultimate state(δ_{max}), and failure modes are given in the table.

3.1 Parameter Analysis

The load-displacement curves of a C-type specimen(C15W-12B), one with flange diaphragms and unreinforced one are compared in Fig. 4. This figure shows that C-type connection which is much simpler than the flange diaphragm type can provide almost the same stiffness and strength by increasing the stiffener thickness by 25%.

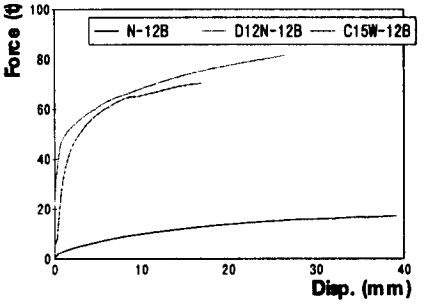

Fig. 4 Effect of reinforcement at connection

Fig. 5 indicates that the eccentricity of the beam flange from the column centerline increases the strength and ductility by transferring the tensile force from the beam flange directly to the side stiffener.

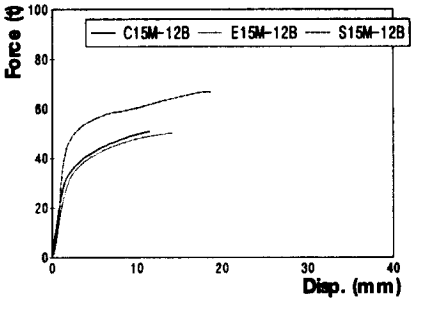

Fig. 5 Strength increase due to eccentricity of beam flange

The increase in the width and thickness of stiffeners increased the strength significantly as shown in Figs. 6 and 7. This is due to that the shear capacity of the stiffener is proportional to its cross sectional area.

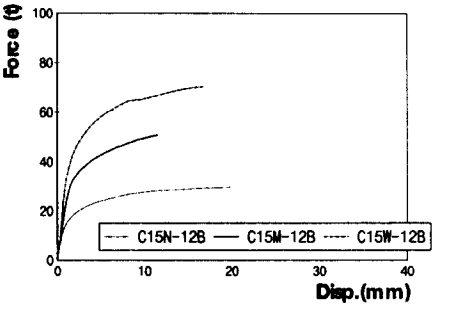

(a) C TYPE

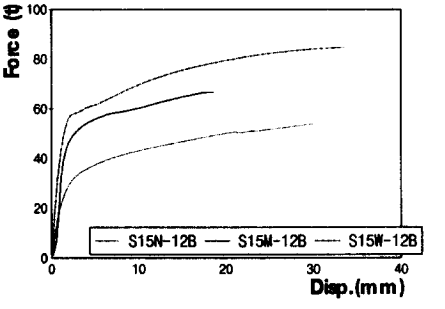

(a) S TYPE

Fig. 6 Effect of stiffner width

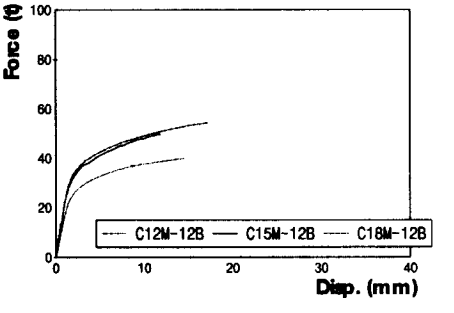

(a) C TYPE

Fig. 7 Effect of stiffner thickness(continued)

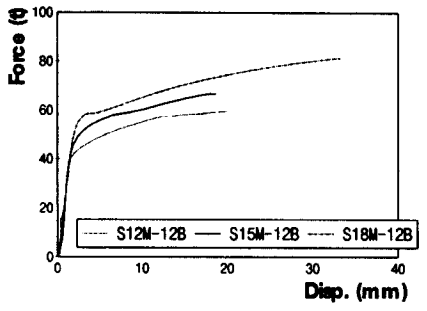

(b) S TYPE

Fig. 7 Effect of stiffner thickness

The strength and ductility were improved by increasing the beam flange width but the effect was not significant as shown in Fig. 8. Similar trends were found for E and S type connections.

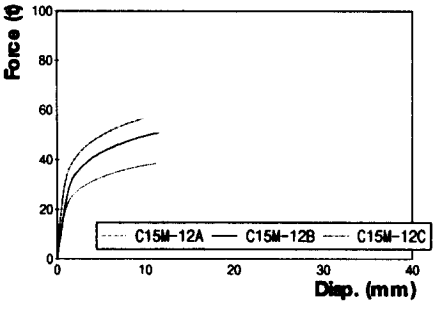

C TYPE

Fig. 8 Effect of beam flange width

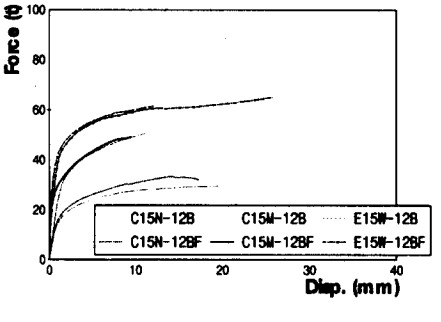

Fig. 9 Effect of concrete filling

The concrete filling in the tube did not increase the strength, though ductility was improved (Fig. 9). This is due to the separation of the tube from the concrete.

The width of side stiffner influenced the strength, but the change was not significant(Fig. 10).

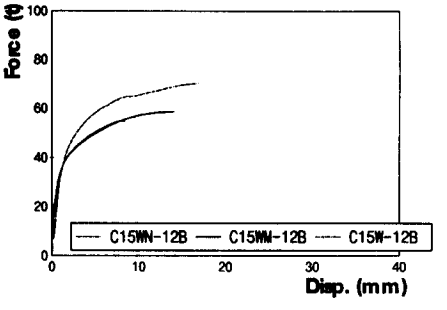

Fig. 10 Effect of side stiffner thickness

3.2 Strain Distribution in Beam Flange

The strain distribution in the beam flange is shown in Fig. 11. The stress concentration is high at the edges of the beam flange and the increase in the stiffener width reduces the strain concentration.

This Figure also shows that most of the flange force is directly transferred to the side stiffener in the S-type specimens.

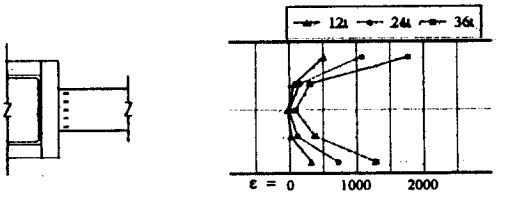

(a) C15M-12B

Fig. 11 Strain distribution in beam flange (continued)

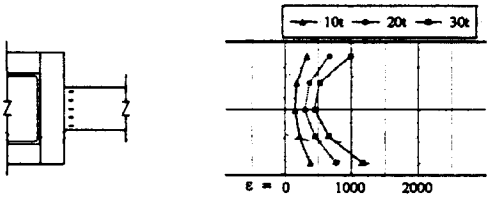

(b) C15W-12B

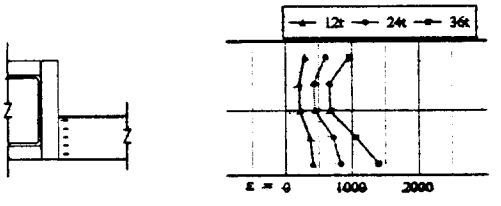

(c) S15M-12B

Fig. 11 Strain distribution in beam flange

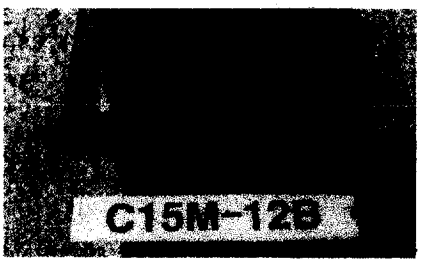

(a) C TYPE

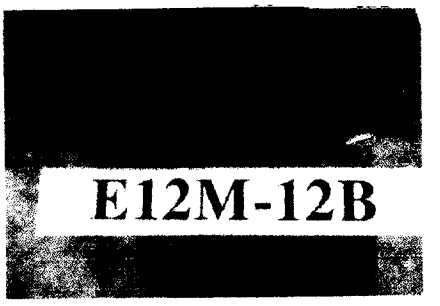

(b) E TYPE

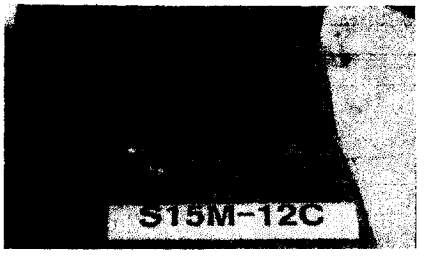

(c) S TYPE

Fig. 12 Typical failure modes

3.3 Failure Mode

The maximum load-carrying capacity was reached when a crack occurred and most of the specimens failed abruptly with noise. The crack began at the end of the weld connecting the beam flange to the tube and propagated along the weld or in 30° ~ 40° direction from the weld.

The specimens which were designed to reach their maximum capacity by the full yielding of the beam flange failed when the flange fractured. Typical failure mode of each type is shown in Fig. 12.

4. Prediction of Ultimate Strength

Several analytical approaches have been proposed for predicting the ultimate strength of the H beam-to-rectangular tube column connections[3,4]. These approaches are based on the yield line mechanism and the principle of virtual work. In this study, a similar approach is used to derive a simplified formula to determine the ultimate capacity.

4.1 C-Type Specimen

The yield line mechanism of the C-type specimen is shown in Fig. 13. An analytical procedure for predicting ultimate strength is established using the principle of virtual work. When there is a displacement, δ, in the beam flange, the external work done by P is

$$W_E = P \cdot \delta \tag{1}$$

The internal works are computed along the yield lines.

Then, the total internal work is

$$W_I = 2(W_{AA} + W_{AA'} + W_{BB} + W_{BB'}) + 4W_{AB} + W_{SD} \tag{2}$$

where W_{SD} is the work done by the shear deformation of the stiffener.

From the principle of virtual work, $W_I = W_E$, we have

$$p = 4M_p\left(\frac{b_c}{x} + \frac{2x}{m} + \frac{t_d}{m}\right) + \frac{2\sigma_{wd}t_d h_d}{\sqrt{3}} \tag{3}$$

From the condition of minimizing P, the distance x is given as

$$x = \sqrt{\frac{b_c m}{2}} \tag{4}$$

Then, the ultimate strength can be evaluated by substituting x into Eq.(3).

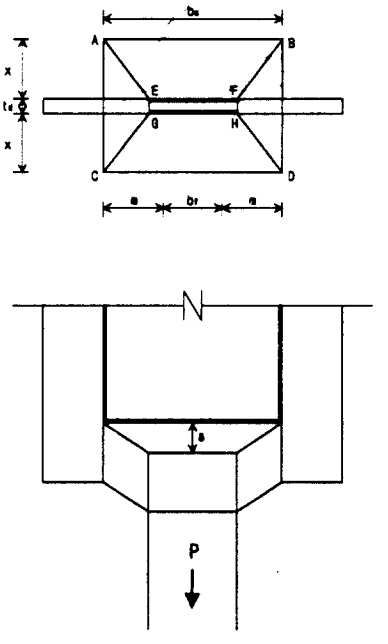

Fig.13 Assumed mode of deformation at connection (C TYPE)

4.2 E-Type Sspecimen

Considering the localized failure of the beam flange near the side face of the tube column, the yield line mechanism is assumed as shown in Fig. 14. Then, the external work done by P is

$$W_E = P \cdot \delta - \sigma_{yf} t_f y \frac{\delta}{2} \tag{5}$$

and the total internal work is

$$W_I = 2(W_{AA'} + W_{CC'} + W_{AC} + W_{A'C'}) + W_{AB} + W_{A'B'} + W_{CD} + W_{C'D'} + W_{SD} \tag{6}$$

From the principle of virtual work,

$W_I = W_E$, we have

$$p = 2M_p(2x + t_d)\left(\frac{1}{y} + \frac{1}{m}\right) + 4M_p b_c / + \frac{2\sigma_{ud} t_d h_d}{\sqrt{3}} + \frac{\sigma_{yf} t_f y}{2} \quad (7)$$

From the condition of minimizing p, $\partial p/\partial x = 0$, $\partial p/\partial y = 0$, we have

$$y = \frac{mx^2}{b_c m - x^2}$$
$$2x^5 + \left(t_d - \frac{m^2 \sigma_{yf} t_f}{4M_p}\right)x^4 - mb_c x \times (4x^2 + 2t_d x - 2mb_c) + m^2 b_c^2 t_d = 0 \quad (8)$$

After finding x and y by numerical method in Eq. (8), the ultimate strength can be evaluated from Eq.(7).

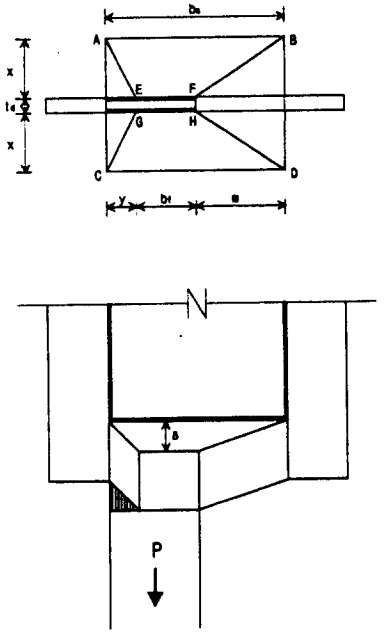

Fig.14 Assumed mode of deformation at connection (E TYPE)

4.3 S-Type Specimen

The deformation mode is assumed as shown in Fig. 15. The calculation procedure is similar to that of E-type except p expressed as

$$p = 2M_p(2x + t_d)\left(\frac{1}{y} + \frac{1}{m}\right) + 4M_p b_c + \frac{2\sigma_{ud} t_d h_d}{\sqrt{3}} + \frac{\sigma_{yf} t_f y}{2} + \left(h_d \frac{+ t_c}{2}\right)\sigma_{yf} t_f \quad (9)$$

where, x and y are computed from Eq. (8).

In the following section, ultimate strength predicted from the equations derived here is compared with the experimental values.

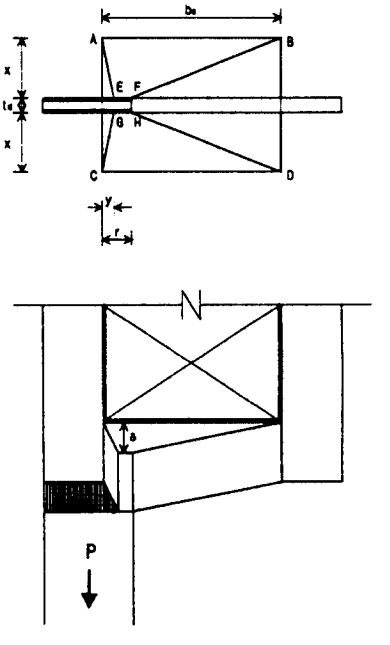

Fig.15 Assumed mode of deformation at connection (S TYPE)

5. Comparison of Experimental and Analytical Results

Fig. 16 shows that the ultimate strengths calcualted by the formula(P_{cal}) agree well with the experimental values(P_{max}). The predicted ultimate strengths were mostly within ±10% error for the C-type and S-type specimens.

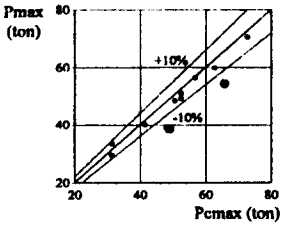

(a) C TYPE

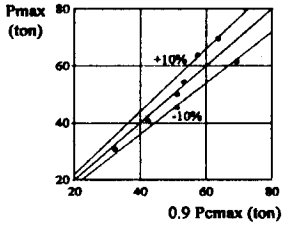

(b) E TYPE

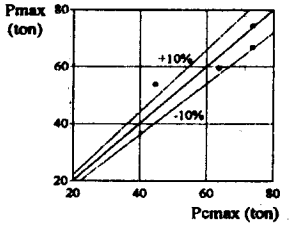

(c) S TYPE

Fig. 16 Prediction of ultimate load

However, the formula overestimated the ultimate strength for the E-type. This is due to the premature failure at the end of the beam flange near the corner of the tube. The ultimate strength of the E-type is in good agreement with the calculated value mutiplied by a factor of 0.9.

The experimental yield strength P_y obtained from the tangent with one third of initial slope of the load-displacement curve showed a proportional relation with the predicted ultimate load. Taking half of the predicted values approximates the yield strength with the error of 10% or less as shown Figure 17.

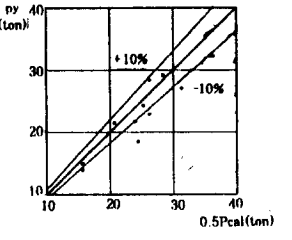

(a) C TYPE

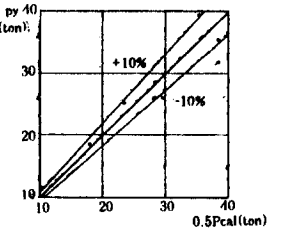

(b) E TYPE

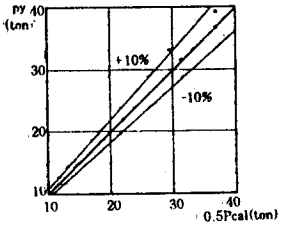

(c) S TYPE

Fig. 17 Yield load prediction

6. Conclusion

A moment connection with external stiffners was proposed. A formula to predict the ultimate strength of the connection was derived based on the yield line mechanism. Experimental investigation was performed to determine the applicability of the connection type and the strength formula. The findings of this study are summarized as follows:

- The proposed connection type is much simpler than the flange diaphragm type but it can provide almost the same stiffness and strength.
- The ultimate strengths computed by the formula agreed well with the experimental values.
- The experimental yield strengths obtained from the tangent with one third of initial slope of the load-displacement curve are in good agreement with the calculated ultimate strengths multiplied by a factor of 0.5.
- The applicability of the E-type connection is limited due to the premature failure caused by stress concentration

References

(1) Giroux, Y. M., and Picard, "Rigid framing connections for tubular columns", Canadian Journal of Civil Engineering, 1997, 4(2): 134-144

(2) Kato, B., Maeda, Y., and Sakae, K., " Behavior of rigid frame sub-assemblages subjected to horizontal force", Joints in Structural Steelwork, John Wiley and Sons, New York, U.S.A., pp. 1.54-1.73.

(3) Morita, K., "Structural behavior of semi-rigid composite joint," Proceedings of International Symposium on Tubular Structures, 1994, pp349-356.

(4) Blodgett, O. W. 'Design of welded structures'. The James F. Lincoln Arc Welding Foundation, Cleveland, 1972.

(접수일자 : 1997. 12. 19)